

peak shift was in the qualitatively correct direction only for the Morse potential model. Although our flexible TIPS model demonstrated a significant shoulder on the low-frequency side of the stretching band it is not clear why neither of the flexible models considered in this work demonstrated a splitting in the main peak of the stretching band. It should be mentioned, however, that no such splitting is in evidence in the inelastic neutron scattering data.²

V. Conclusions

In this work we have described a simple intramolecular potential model useful for describing some aspects of the flexibility of water near standard temperature and pressure. The parameters were fit to give agreement with the ground vibrational state frequencies as measured by experiment and so yield an effective classical intramolecular potential surface for describing systems at temperatures where the ground state may be expected to dominate the vibrational population distribution. By a judicious choice of functional form this model required only the computational effort of a simple collection of harmonic oscillators while yielding environmental shifts in the correct directions and in good qualitative agreement in magnitude with experiment. Harmonic normal-mode analysis of clusters revealed that our simple coupled harmonic force field is capable of reproducing environmentally induced frequency shifts previously only obtained with complicated intramolecular potential forms.

Using the sort of model we have presented, it is possible to perform a full quasi-harmonic-mode analysis on the dynamic liquid-state trajectories.²⁸ Such an analysis should yield a direct

description of the eigenvectors associated with high-frequency motions. This model is not as accurate for the assignment and exploration of the quantum mechanical overtone spectral structure of water, such as the features associated with frequencies in excess of 4000 cm⁻¹ or of hot clusters such as those generated in a predissociation experiment, as other models which have been extensively optimized for this purpose.⁵ However, the essentially harmonic nature of the potential form used guarantees that the ground-state quantum mechanical frequencies will not differ significantly from those found in our classical normal-mode calculation. Our model's ability to accurately reproduce certain aspects of the vibrational motions of neat water in a wide variety of applications is sufficiently encouraging that it should be a useful tool for studying frequency shifts in ionic solutions and solutions containing highly polar molecules such as zwitterions. In addition this model should be useful in large solute aqueous simulations where high efficiency combined with qualitative accuracy is needed.

Acknowledgment. We are grateful to the Robert A. Welch Foundation for support of this work and the Texas Advanced Research Projects coordinating board for page charges. HYDRA by Rod Hubbard was used to make Figure 2. We also thank the University of Houston Computing Center for generous amounts of AS9000n computer time and Dr. J. Madura and Prof. A. McCammon for a careful reading of this manuscript.

Registry No. H₂O, 7732-18-5.

(28) Dang, L. X.; Pettitt, B. M., work in progress.

Thermodynamic Properties of Supercooled Water at 1 atm

Robin J. Speedy

Chemistry Department, Victoria University of Wellington, Wellington, New Zealand
(Received: December 9, 1986)

The measured thermodynamic properties of liquid water in the temperature range -38 to 150 °C at 1 atm are represented precisely by a set of self-consistent equations which are singular at a temperature $T_s = -46$ °C. Comparison of the estimated properties of liquid water at T_s with the properties of vitreous solid water prepared by rapidly quenching liquid water to 77 K gives good agreement for the densities but a contradiction in the case of the enthalpy.

1. Introduction

Interest in the properties of supercooled water is stimulated by the rapid quenching experiments of Brüggeler and Mayer,¹ Mayer,² and Dubochet³ which produce an amorphous solid substance by the very rapid (10⁶ K/s) cooling of small samples of liquid water to 77 K. Other amorphous solid waters have been prepared by vapor deposition⁴ and recently Mishima, Calvert, and Whalley⁵ have produced two distinct amorphous solid waters by compressing ice.

According to the stability limit conjecture^{6,7} the free energy surface for liquid water terminates at a line of stability limits $T_s(p)$ in the p, T plane at which the isothermal compressibility, κ_T , extrapolates to infinity. One implication of the conjecture is that the characteristic times for structural relaxation processes would

also diverge as the stability limit is approached. If that is so, then the rapidly quenched liquid samples would become structurally arrested^{7,8} in a state which corresponds to that of liquid water near $T_s(1 \text{ atm}) = -46$ °C⁸ and may be quite different from the amorphous solid samples prepared by vapor deposition. It is of interest, then, to estimate the density and enthalpy of supercooled water near -46 °C and to compare them with the densities and enthalpies of the various amorphous solids.

Sections 2 and 3 discuss the reliability of the experimental measurements on supercooled water and the justification for the particular forms⁹ chosen for their extrapolation to -46 °C. The results of the extrapolation are presented in section 4 and the estimated density and enthalpy of supercooled water at -46 °C are compared with those of amorphous solid water in section 5.

2. The Measurements

Three main sets of measurements on supercooled water are used in the analysis. Angell, Sichina, and Oguni¹² measured the heat capacity, C_p , for water in emulsions to -37 °C with a precision

(1) Brüggeler, P.; Mayer, E. *Nature (London)* **1980**, *288*, 596.

(2) Mayer, E. *J. Microsc.* **1985**, *140*, 3.

(3) Dubochet, J.; McDowell, A. W. *J. Microsc.* **1981**, *124*, RP3.

(4) Mishima, O.; Calvert, L. D.; Whalley, E. *Nature (London)* **1984**, *310*, 393; **1985**, *314*, 76.

(5) Sceats, M. G.; Rice, S. A. In *Water, a Comprehensive Treatise*; Franks, F., Ed.; Plenum: New York, 1981; Vol. 7, Chapter 2.

(6) Speedy, R. J.; Angell, C. A. *J. Chem. Phys.* **1976**, *65*, 851.

(7) Speedy, R. J. *J. Phys. Chem.* **1982**, *86*, 982.

(8) Cornish, B. D.; Speedy, R. J. *J. Phys. Chem.* **1984**, *88*, 1888.

(9) Speedy, R. J. *J. Phys. Chem.* **1982**, *86*, 3002.

(10) Hare, D. E.; Sorensen, C. M. *J. Chem. Phys.* **1986**, *84*, 5085.

TABLE I: Measured Density¹⁰ ρ , Heat Capacity¹² C_p , and Isothermal Compressibility⁶ κ_T of Supercooled Water and Their Residuals When Fitted to Eq 11 and 12 with the Constants Listed in Table II

$T/^\circ\text{C}$	$\rho/\text{g cm}^{-3}$	residual, ppm	$T/^\circ\text{C}$	$C_p/\text{J K}^{-1} \text{mol}^{-1}$	residual	$T/^\circ\text{C}$	$\kappa_T/10^{-6} \text{bar}^{-1}$	residual
-34.2	0.978 40	0	-37.1	102.7	0.3	-26.1	71.3	0.3
-30.04	0.984 72	0	-36.1	99.0	-0.3	-26.1	70.6	-0.4
-25.19	0.990 10	7	-35.1	96.5	-0.1	-23.9	66.1	-2.0
-20.19	0.993 90	0	-34.1	94.4	0.1	-23.6	69.5	1.8
-15.28	0.996 52	-3	-33.1	92.3	0.0	-22.3	66.7	0.4
-10.34	0.998 25	-9	-31.1	88.4	-0.4	-21.1	64.5	-0.5
-5.35	0.999 36	-6	-28.1	85.2	-0.6	-20.3	64.6	0.3
-0.28	0.999 89	-1	-23.1	81.4	-0.6	-9.3	56.2	-0.1
4.61	1.000 00	13	-18.1	78.8	0.4	-1.1	52.7	0.3
						10.0	47.9	-0.7
						20.0	45.9	-0.1

TABLE II: Constants in Eq 11 and 12 Which Fit the Data Shown in Table I

	$\alpha \times 10^6/\text{K}^{-1}$	$\kappa_T \times 10^6/\text{bar}^{-1}$	$C_p/\text{J K}^{-1} \text{mol}^{-1}$	$\rho_s/\text{g cm}^{-3}$
$B_x^{(0)}$	1796	15.6	42.9	0.9176
ice (0 °C)	150	13	37.6	0.9159
C_x	-824	16.4	11.77	

$$\frac{dp_s}{dT} / \text{bar K}^{-1} \frac{C_a}{C_x} = 50.3 \left(\frac{C_c}{C_s T_s V_s} \right)^{1/2} = 40.3 \text{ eq 1, } 39.2 \pm 2.4$$

of about 1%. Speedy and Angell⁶ measured the isothermal compressibility, κ_T , in 20 μm diameter capillaries to -26°C with a precision of about 2%. Hare and Sorenson¹⁰ measured the density, ρ , in 25 μm diameter capillaries to -34°C . Their mean results have a precision of better than 10 parts per million (ppm) (Table I) but in view of the larger variations between different workers, Hare and Sorenson suggest that their results may differ from those of bulk water by a few hundred ppm. Their densities are 300 ppm larger than Zhelezynis¹³ values near -34°C .

Leyendekkers and Hunter¹¹ have argued that the above measurements need to be corrected for surface tension effects. Their analysis is incorrect and misleading so a brief analysis of the surface tension effect is given here.

The effect of a surface tension γ on a spherical drop of radius r is to increase the pressure acting on the material in the drop by $2\gamma/r$. The density of the material will be increased by $(\partial\rho/\partial p)_T 2\gamma/r > 0$ and its heat capacity C_p will be increased by $(\partial C_p/\partial p)_T 2\gamma/r$. For water near 0°C $(\partial C_p/\partial p)_T < 0$ so the surface tension acts to reduce the apparent capacity of small drops relative to that of bulk water.

The drops of water in the emulsions used by Angell, Sichina, and Oguni¹² are 1–5 μm in diameter. Their surface tension is determined by the surfactant (Span 65) which stabilizes the surface and therefore reduces the surface tension to a value smaller than that associated with the water–gas interface which is $\gamma = 7.20 \times 10^{-2} \text{ N m}^{-1}$ at 25°C . An upper bound on $2\gamma/r$, estimated by taking $r = 1 \mu\text{m}$ and $\gamma = 7.2 \times 10^{-2} \text{ N m}^{-1}$, is $2\gamma/r < 1.4 \text{ atm}$. This would increase the density of the water at 25°C by less than 70 ppm, and its heat capacity would be reduced by less than 0.02%. Leyendekkers and Hunter¹¹ argue that the heat capacities reported by Angell et al. are up to 20% too large because Angell et al. did not correct their data for the surface tension effect. The above discussion shows, however, that the surface tension would reduce rather than increase the apparent heat capacity and that the effect is a thousand times smaller in magnitude.

It is well-known that the attraction between water and glass causes water to rise, against gravity, in a small capillary. The pressure and density of the water in the capillary are therefore reduced. For small capillaries the radius of curvature of the

TABLE III: Fitting Constants in Eq 13 and 14^a

x	$\alpha \times 10^3/\text{K}$	$\kappa_T \times 10^6/\text{bar}^{-1}$	$C_p/\text{J K}^{-1} \text{mol}^{-1}$
C_x	-0.80	20.0	14.2
$B_x^{(0)}$	1.8021803	4.120	25.952
$B_x^{(1)}$	-0.9416980	-1.130	128.281
$B_x^{(2)}$	0.9055070	77.817	-221.405
$B_x^{(3)}$	-0.0579531	-78.143	196.894
$B_x^{(4)}$		54.290	-64.812
max residual	1.2 ppm in density	0.2%	0.03%

^a $\rho_s = 0.920170 \text{ g cm}^{-3}$. $V_s = 19.5616 \text{ cm}^3 \text{mol}^{-1}$. $T_s = 227.1 \text{ K}$. $C_a/C_x = -40.0 \text{ bar K}^{-1}$. $(C_c/(C_s T_s V_s))^{1/2} = -39.98 \text{ bar K}^{-1}$. Equations 13 and 14 were fitted to the smoothed values of the density ρ , κ_T , and C_p given by Kell^{18,20} over the temperature range $0^\circ\text{C} \leq T \leq 150^\circ\text{C}$ with the values of C_x predetermined to satisfy eq 5 and 6 with $dp_s/dT = -40 \text{ bar K}^{-1}$. The residuals are smaller than the rated absolute error in each case. Extrapolation of these equations into the supercooled region accurately predicts the measured values of C_p , κ_T , and ρ as shown in Figures 1–3.

meniscus is the same as the radius of the capillary bore and the pressure is reduced by $2\gamma/r$. On that basis, water in a 10 μm radius capillary (with a liquid–vapor interface) will be less dense than bulk water by $(\partial\rho/\partial p)_T 2\gamma/r$, or about 7 ppm.

There are significant differences between densities measured in 4¹⁴, 10¹⁰, and 25¹¹ μm diameter capillaries but the apparent density is greatest in the small capillaries and this cannot be explained by the surface tension effect as Leyendekkers and Hunter¹¹ claim. Their estimates of the correction are orders of magnitude larger than those estimated here. They are also of the opposite sign.

That the surface tension is not an important factor should not be taken to imply that the κ_T , C_p , and ρ data are reliable. There are some capillary size effects which have not been explained.^{10,11} One possibility is that there is a wetting layer of water on the surface of the unfilled part of the capillary whose thickness increases as the temperature is reduced.¹⁵

Two other pieces of evidence needed in the analysis are the location of T_s (1 atm) and the slope dp_s/dT of the locus of T_s .

The thermodynamic data do not, by themselves, provide a precise estimate of T_s . α , C_p , and κ_T can be fitted to equations which diverge at different temperatures depending on how background corrections are made.^{10,11} In any case, a determination of T_s (1 atm) which is independent of the data to be analyzed is preferable.

A study of the electrical conductivity of dilute electrolyte solutions was undertaken to determine T_s .⁸ Since a diverging compressibility implies diverging relaxation times, the point at which solution conductivities extrapolate to zero locates T_s . The conductivities show a much greater temperature dependence than the thermodynamic properties; they can be measured precisely to low temperatures and no background corrections are needed. The most precise estimate of T_s is obtained from the proton conductance,⁸ λ_{H^+} , which varies linearly with T

$$\lambda_{H^+} = A(T - T_s), \quad -32^\circ\text{C} < T < 45^\circ\text{C}$$

(15) Beaglehole, D., private communication.

(11) Leyendekkers, J. V.; Hunter, R. J. *J. Chem. Phys.* **1985**, *82*, 1440, 1447.

(12) Angell, C. A.; Sichina, W. J.; Oguni, M. *J. Phys. Chem.* **1982**, *86*, 998.

(13) Zheleznyi, B. V. *Russ. J. Phys. Chem.* **1969**, *43*, 1311.

(14) Schuffe, J. A.; Venugopalan, M. *J. Geophys. Res.* **1967**, *72*, 3271. Schuffe, J. A. *Chem. Ind.* **1965**, 690.

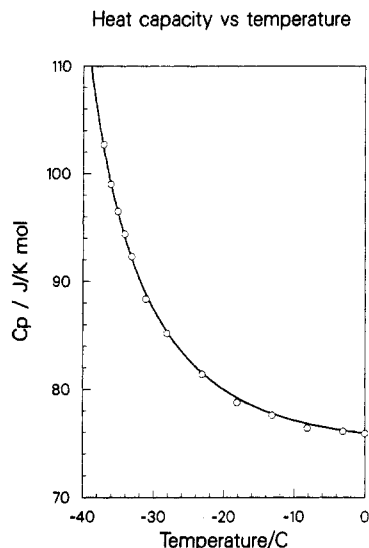


Figure 1. The heat capacity C_p of supercooled water at 1 atm. Circles show the experimental results of Angell, Sichina, and Oguni. The line represents eq 13 with the parameters given in Table III.

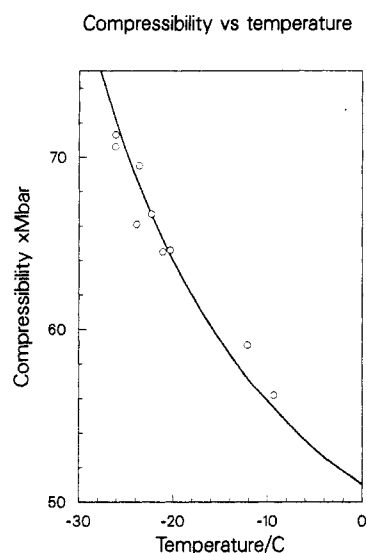


Figure 2. The isothermal compressibility of supercooled water at 1 atm. Circles represent the experimental results of Speedy and Angell.⁶ The line represents eq 13 with the parameters given in Table III.

with $T_s = -46 \pm 2^\circ\text{C}$. This value of T_s is consistent with values determined in a variety of other ways, but is more precise.

Lang and Lüdemann's¹⁶ measurement of the spin-lattice relaxation time T_1 for water in emulsions at high pressure provide the best estimates of $T_s(p)$. Their estimates are summarized in Table III and Figure 4 of ref 7. The data in the range $-750 \text{ atm} < p < 1500 \text{ atm}$ were fitted by linear regression to

$$p_s(T) = (dp_s/dT)(T - T_s)$$

to yield $T_s = -46^\circ\text{C}$ and

$$dp_s/dT = -39.2 \pm 2.4 \text{ atm/K} \quad (1)$$

The error quoted is the standard statistical error in the linear regression estimate of the slope.

3. Consistency Relations

In this section the postulates and assumptions which underlie the relations needed in the data analysis are stated. Derivations have been published^{7,9,17} previously and will not be reproduced.

Density vs temperature

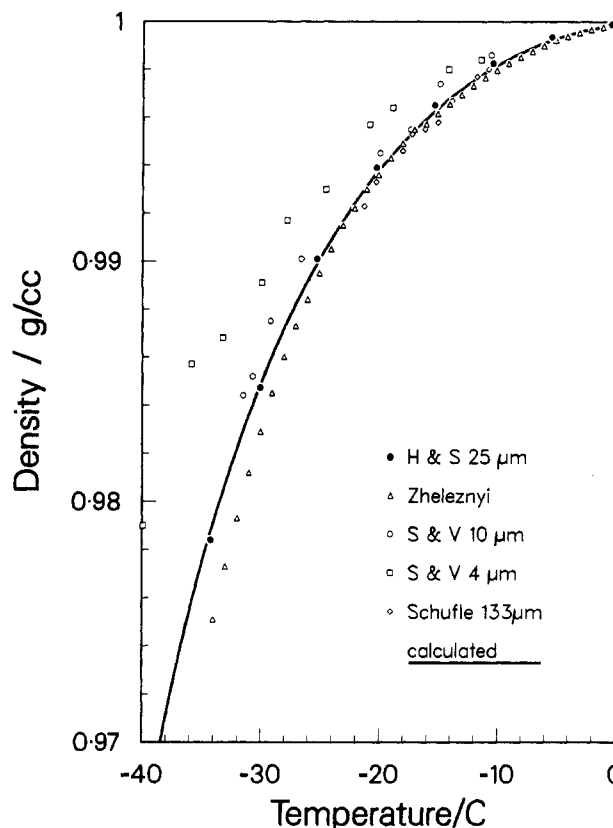


Figure 3. The density of supercooled water at 1 atm: ●, Hare and Sorensen¹⁰ 25- μm capillaries; Δ , Zheleznyi,¹³ ○, Schufle and Venugopalan¹⁴ 10- μm capillaries; \square , Schufle and Venugopalan¹⁴ 4- μm capillaries; \diamond , Schufle,¹⁴ 133- μm capillaries; —, eq 14 with the parameters given in Table III.

A fuller discussion is given in ref 9.

The central postulate^{6,7} is that water behaves as though there exists a line $T_s(p)$ at which the isothermal compressibility κ_T diverges. $T_s(p)$ is called the stability limit temperature.

There is some doubt⁹ as to the meaning of thermodynamic properties near $T_s(p)$ but they can be taken to be defined by thermodynamically self-consistent extrapolations from nearby regions where they are well-defined. It is assumed that thermodynamic arguments are applicable near T_s .

Straightforward thermodynamic arguments^{7,17} show that if

$$\kappa_T \rightarrow \infty \text{ as } T \rightarrow T_s(p)$$

then

$$\alpha \rightarrow (dV_s/dT)/V_s + (dp_s/dT)\kappa_T \rightarrow \pm\infty \text{ as } T \rightarrow T_s(p)$$

and

$$C_p \rightarrow T(dS_s/dT) + T_s V_s (dp_s/dT)^2 \kappa_T \rightarrow \infty \text{ as } T \rightarrow T_s(p) \quad (2)$$

where the derivatives are taken along the line $T_s(p)$.

With X symbolizing κ_T , α , or C_p a plausible representation of the temperature dependence is^{7,17}

$$X = B_x + C_x \epsilon^{-\gamma_x} \quad (3)$$

where $\epsilon = (T/T_s(p) - 1)$. $C_x \epsilon^{-\gamma_x}$ represents the most strongly diverging term and B_x collects the background terms, which may include weaker divergences and the constants $(dV_s/dT)/V_s$, $T(dS_s/dT)$ which appear in relations 2.

Relations 2 indicate that α , C_p , and κ_T are asymptotically proportional to each other as $T \rightarrow T_s$, which implies that

(16) Lang, E. W.; Lüdemann, H.-D. *Angew. Chem., Int. Ed. Engl.* **1982**, *21*, 315.

(17) Ahlers, G. In *The Physics of Liquid and Solid Helium*; Benemann, K. H., Ketterson, J. B., Eds.; Wiley: New York, 1976; Chapter 2.

TABLE IV: Values of the Thermodynamic Properties of Supercooled Water Calculated from Eq 13 and 14 with the Constants Listed in Table III^a

$T/^{\circ}\text{C}$	$\alpha \times 10^6/\text{K}^{-1}$	$\kappa_T \times 10^6/\text{bar}^{-1}$	$C_p/\text{J K}^{-1} \text{mol}^{-1}$	$\Delta_s^1 H/\text{kJ mol}^{-1}$	$\Delta_s^1 S/\text{J mol}^{-1}$	$\Delta_s^1 G/\text{J mol}^{-1}$	density/ g cm^{-3}
-46.0	$-\infty$	∞	∞	3.04	9.76	823	0.920 17
-45.0	-10255.9	305.5	240.49	3.46	11.62	812	0.940 93
-40.0	-3135.9	127.2	116.55	4.06	14.22	746	0.965 70
-35.0	-1861.7	95.1	96.19	4.42	15.74	672	0.977 37
-30.0	-1252.5	79.7	87.46	4.71	16.94	590	0.984 86
-25.0	-880.3	70.4	82.77	4.96	17.97	502	0.990 07
-20.0	-623.8	64.0	79.99	5.192	18.89	410	0.993 76
-15.0	-434.0	59.4	78.25	5.409	19.74	314	0.996 37
-10.0	-286.3	55.9	77.13	5.616	20.54	213	0.998 15
-5.0	-167.3	53.1	76.40	5.815	21.29	108	0.999 28
0.0	-68.7	51.0	75.93	6.008	22.00	0	0.999 86

^a The values of $^{22} \Delta_s^1 S(T_m) = 22 \text{ J K}^{-1} \text{mol}$ and $^{21} C_{p,1} = 31.869 + 29.5\epsilon$ are also used in the calculation of $\Delta_s^1 H$, $\Delta_s^1 S$, and $\Delta_s^1 G$.

$$\gamma = \gamma_\kappa = \gamma_\alpha = \gamma_{C_p} \quad (4)$$

and that

$$C_\alpha/C_\kappa = (dp_s/dT) \quad (5)$$

$$C_{C_p}/C_\kappa = T_s V_s (dp_s/dT)^2 \quad (6)$$

Furthermore, one has

$$\gamma < 1 \quad (7)$$

because a value $\gamma \geq 1$ would imply, from integrating eq 3, that the volume and enthalpy would diverge at T_s . For example, the enthalpy H at T_s is

$$H(T_s) = H(T_m) + \int_{T_m}^{T_s} B_{C_p} dT + \frac{T_s}{1-\gamma} \epsilon^{1-\gamma}, \quad \gamma \neq 1 \quad (8)$$

and if $\gamma > 1$ the last term diverges, implying that it would take the removal of an infinite amount of heat to cool water to T_s . Similarly, if $\gamma = 1$, $H(T)$ diverges logarithmically as $T \rightarrow T_s$, so the only sensible possibility is eq 7.

Incidentally, while it clearly makes no sense to violate eq 7, many empirical equations which have been used to represent the properties of water and other liquids do so. The Tait equation¹⁸ is a familiar example. Kell's expression for the compressibility of water at 1 atm (eq 6 of ref 18) is another:

$$\kappa_T = \sum_{n=0}^5 a_n t^n / (1 + 21.65928 \times 10^{-3} t) \quad (9)$$

where the a_n are constants and $t = T/\text{K} - 273$. Equation 9 implies that $\kappa_T \rightarrow \infty$ as $t \rightarrow -1/21.659 \times 10^{-3} \text{ }^{\circ}\text{C} = -46.16 \text{ }^{\circ}\text{C}$, in excellent agreement with other estimates of T_s . However, eq 9 also implies, through eq 2, that $-\alpha$ and C_p diverge too, and since $\gamma = 1$ in eq 9 the volume and enthalpy also diverge. Kell's equation for the density (eq 5 of ref 18) of water at 1 atm implies that the volume diverges at $-55 \text{ }^{\circ}\text{C}$. It should not be surprising then that these very precise representations of the properties of bulk water above $0 \text{ }^{\circ}\text{C}$ disagree with experimental measurements at lower temperatures.

A mean field value of γ is defined by the extra assumption⁹ that the Helmholtz potential $A(V, T)$ is an analytic function of V and T . If that assumption is valid at $T_s(p)$ then it follows, as detailed in ref 9, that

$$\gamma = 1/2 \text{ along an isobar} \quad (10)$$

Since data cannot be obtained close enough to T_s to determine an alternative value, eq 10 is used in preference to regarding γ as a fitting constant.

4. Results

Without measurements close to T_s there is no unique way to establish the background terms B_x in eq 3. Angell and co-workers

discuss experimental routes to the background terms.¹⁹ Sufficiently close to T_s the strongly divergent term will vary much more rapidly than B_x so that, over a limited temperature range, the B_x can be approximated by constants. In that case

$$X = B_x^{(0)} + C_x \epsilon^{-1/2} \quad (11)$$

where $B_x^{(0)}$ is constant.

For the case $X = \alpha$ integration of eq 11 gives the density

$$\rho = \rho_s \exp(-T_s \{B_\alpha^{(0)} \epsilon + 2C_\alpha \epsilon^{1/2}\}) \quad (12)$$

and since it is ρ that is measured directly, rather than α , eq 12 was fitted to obtain the value of $\rho_s B_\alpha^{(0)}$, and C_α shown in Table II.

The data sets fitted to eq 11 and 12 are listed in Table I and the fitting constants in Table II. The temperature range chosen was that over which the assumption that $B_x^{(0)}$ is constant provides a fit to within the precision of the data.

Table II also lists the corresponding properties of ice at $0 \text{ }^{\circ}\text{C}$ to compare with the background terms $B_x^{(0)}$ and ρ_s . The density ρ_s at T_s is, to within the error of extrapolation, that of ordinary ice. The background heat capacity and compressibility terms are also icelike but the expansivity term is quite different.

The last line of Table II invokes the consistency tests provided by eq 5 and 6 according to which the three different methods of calculating dp_s/dT should yield the same value. The last two values are in good agreement but the first is 20% higher. The fact that the three quite independent estimates of dp_s/dT are nearly the same is a strong indication in favor of the stability limit conjecture.

To establish that the experimental measurements are consistent with the relations given in the last section, and also to provide precise representations of the properties of water which are self-consistent, the background terms in eq 3 were represented by polynomials in $\epsilon = (T - T_s)/T_s$ so that

$$X = \sum_{n=0} B_x^{(n)} \epsilon^n + C_x^{-1/2} \quad (13)$$

and

$$\rho = \rho_s \exp\left(-T_s \left\{ \sum_{n=0} \frac{1}{n+1} B_\alpha^{(n)} \epsilon^{n+1} + 2C_\alpha \epsilon^{1/2} \right\}\right) \quad (14)$$

Consistency with eq 5 and 6 was forced by arbitrarily choosing $C_\kappa = 20 \times 10^{-6} \text{ bar}^{-1}$, which, together with the round figure value of $dp_s/dT = -40 \text{ bar K}^{-1}$ from eq 1, determines the values of C_α and C_{C_p} shown in Table III.

Precise values of κ_T , C_p , and ρ at 1 atm, obtained from measurements on bulk samples in the temperature range $0 \text{ }^{\circ}\text{C} < T < 150 \text{ }^{\circ}\text{C}$ are smoothed and tabulated by Kell.^{18,20} The background terms $B_x = X - C_x \epsilon^{-1/2}$ and $\ln \rho + 2T_s C_\alpha \epsilon^{1/2}$ were fitted to those data, taken at intervals of $10 \text{ }^{\circ}\text{C}$, by regression, to determine the $B_x^{(n)}$ listed in Table III. Sufficient terms were included to ensure that the residuals were smaller than the rated accuracy of the data.^{18,20}

(18) Kell, G. S. In *Water, a Comprehensive Treatise*; Franks, F., Ed.; Plenum: New York, 1972; Vol. 2, Chapter 10.

(19) Oguni, M.; Angell, C. A. *J. Chem. Phys.* **1980**, *73*, 1948.

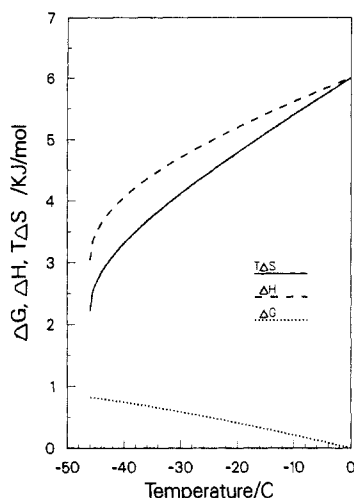


Figure 4. $\Delta^l G$, and $\Delta^l H$, and $T\Delta^l S$ for supercooled water at 1 atm, calculated by using eq 13 for $C_{p,w}$ with the parameters given in Table III.

Note that none of the measurements made on capillary or emulsion samples and no measurements below 0 °C were included in the fitting procedure. The only influence that measurements below 0 °C have on the fitting procedure is to guide the initial choice of C_k and to give the independent estimates of T_s and dp_s/dT . The resulting equations are robust in the sense that varying C_k by 20% or so has little effect on the conclusions.

Figures 1–3 show that the experimental measurements on supercooled water are precisely represented by eq 13 and 14 with the constants listed in Table III.

Values of $\Delta^l H$, $\Delta^l S$, and $\Delta^l G$, the enthalpy, entropy, and Gibbs functions of supercooled water relative to ice, were calculated by integrating eq 13 for C_p , using for ice the expression

$$C_{p,i}/\text{J K}^{-1} \text{mol}^{-1} = 31.869 + 29.5\epsilon$$

which represents the measurements of Giauque and Stout.²¹ The results are listed in Table IV and illustrated in Figure 4.

The values of $\Delta^l G$ can be compared with estimates made by Leyendekkers and Hunter¹¹ by extrapolating the properties of bulk water to -40 °C, and by using Angell, Oguni, and Sichina's heat capacity measurements on emulsified samples. The values in Table IV agree with their estimates for bulk water to -30 °C to within 1 J mol⁻¹ and become 3 J mol⁻¹ lower than theirs at -40 °C. In contrast, it is claimed in ref 11 that values of $\Delta^l G$ calculated from Angell, Oguni, and Sichina's heat capacity measurements are systematically, and significantly, higher than bulk water values. Since our equation was fitted to bulk water and also clearly represents Angell, Oguni, and Sichina's C_p data precisely, as shown in Figure 1, the contradiction must be computational in origin. My conclusion is that there is no evidence to indicate that the measurements are unreliable.

5. Discussion

An important conclusion to be drawn is that there is no inconsistency between the measured values of C_p , κ_T , and the densities reported by Hare and Sorensen. Nor is there any inconsistency between those measurements and extrapolations of

the properties of bulk water measured above 0 °C. Such discrepancies as have been claimed¹¹ probably arise from the methods of extrapolation rather than from any errors in the measurements.

A second conclusion is that the measurements are consistent with the stability limit conjecture and with the locus $T_s(p) = -46$ °C - $p/40$ bar °C⁻¹ determined independently from transport data. Furthermore, they are consistent with the assumption that the Helmholtz potential $A(V, T)$ is analytic near T_s .

Those conclusions give some credence to, although they do not establish, the reliability of the estimates of the density and enthalpy of supercooled water near T_s shown in Table IV. Those values will now be compared with the density and enthalpy of the low-density forms of amorphous solid water prepared by different methods.

The density of the liquid at T_s (1 atm) is, from Table IV, $\rho_s \approx 0.92$ g/cm³ which is close to the density of ice Ih,²² $\rho_i = 0.923$ g cm⁻³ at -46 °C. The density of amorphous solid waters prepared by vapor deposition²³ at 77 K, or by decompressing a higher density form²⁴ at 117 K, is about 0.94 g/cm³, which is close to the density of ice²² at those temperatures. There are sufficient spectroscopic similarities between those amorphous solids and the vitreous solid prepared by quenching liquid water to suggest that the latter has a similar density.^{2,24} That conclusion accords well with the proposal^{7,8} that when liquid water is cooled fast enough to bypass crystallization, structural arrest occurs close to T_s so the structure and density of the vitreous solid is that of water at T_s .

The enthalpy change for the freezing of vitreous solid water to ice Ic at 158 K is²⁵ $\Delta_{wH}^{lc}(158 \text{ K}) = -1330$ J/mol. Values of ΔH for the crystallization of other amorphous solid waters range from ^{24,25} -900 to -1800 J/mol. Those values are much less than the value $\Delta^l H(T_s(1 \text{ atm})) = -3044$ J/mol for the freezing of water to ice Ih, from Table IV. The enthalpy difference between ice Ic and ice Ih is only about²⁶ 50 J/mol and does not bridge the gap. If structural arrest occurs at T_s , then the heat capacity of the vitreous solid, below T_s , should drop to a value near that of ice so that the predicted value of $\Delta_{wH}^{lc} = -3000$ J/mol would not be expected to vary much with temperature below T_s .

There is then a contradiction. The enthalpy of vitreous water is about 1700 J/mol lower than would be expected if its properties corresponded to those of water at T_s . This suggests that some further structural relaxation occurs in the vitreous solid during the quench or when it is annealed at 77 K. If that is the case, then its structure and properties do not correspond to those of liquid water at T_s .

Mayer² has noted some spectroscopic and thermal evidence for the existence of two distinguishable forms of vitrified water whose relative proportions are dependent on the quenching rate. Further studies of these materials may indicate a resolution of the above contradiction.

Acknowledgment. I am grateful to J. V. Leyendekkers, R. J. Hunter, and D. Beaglehole for comments, and C. M. Sorensen and E. Mayer for preprints.

Registry No. H₂O, 7732-18-5.

(22) Eisenberg, D.; Kauzmann, W. *The Structure and Properties of Water*; Clarendon: Oxford, U.K., 1969.

(23) Narten, A. H.; Venkatesh, C. G.; Rice, S. A. *J. Chem. Phys.* **1976**, *64*, 1106.

(24) Handa, P. Y.; Mishima, O.; Whalley, E. *J. Chem. Phys.* **1986**, *84*, 2766.

(25) Hallbrucker, A.; Mayer, E. *J. Phys. Chem.*, preprint.

(26) Harta, P. Y.; Klug, D. D.; Whalley, E. *J. Chem. Phys.* **1986**, *84*, 7009.

(20) Kell, G. S. *J. Chem. Eng. Data* **1967**, *12*, 66.

(21) Giauque, W. F.; Stout, J. W. *J. Am. Chem. Soc.* **1936**, *58*, 1144.